Observations of Transitions Between Stationary States in a Rotating Magnetic Field*

WILLIAM HAPPER, JR.
Palmer Physical Laboratory, Princeton University, Princeton, New Jersey
(Received 20 March 1964; revised manuscript received 3 June 1964)

The stationary states of an atom in a combined static and rotating magnetic field have been investigated by using two frequency transitions in an atomic-beam machine. Very accurate measurements of a strong rf magnetic field may be made by inducing transitions between the stationary states with a small "tickling" rf field. The relaxation of the selection rules associated with the z component of angular momentum makes normally forbidden hyperfine transitions visible.

I. INTRODUCTION

TWO-FREQUENCY transitions have been observed by several investigators in the past,[1,2] and are usually interpreted as multiple quantum processes where the energy and angular momentum for a transition are supplied by two photons. We wish to report on observations involving two frequencies, where one rf field may be thought of as defining stationary states, between which a small secondary rf field causes transitions. The steady-state solutions of an atom in a precessing magnetic field were originally obtained independently by Besset *et al.*,[3] Salwen,[4] and Hack.[5] They are frequently used to analyze single-frequency transitions between hyperfine sublevels of an atom in a magnetic field. While algebraic solutions for a three-level system can be obtained, as was first shown by Blamont and Winter[6] and more recently by Franzen and Alam,[7] the case for an arbitrary number of levels is usually treated with perturbation theory.[3,4] In this work the Hamiltonian matrix in the rotating coordinate system was diagonalized with an electronic computer to obtain eigenvectors and eigenvalues for interpretation of the experimental data. The exact steady-state solutions may be used to solve for the transition probability in a region of overlapping multiple quantum resonances where neither the usual perturbation methods[3–5] for treating multiple quantum resonances, nor the Majorana formula[8] apply.

In this paper we shall think of a strong rf field together with a static magnetic field as playing the role of the homogeneous magnetic field in ordinary rf spectroscopy. By causing transitions with a weak secondary rf field we may investigate the structure of the stationary states. Very accurate measurements of the primary rf magnetic-field strength may be made in this manner. The transitions between stationary states in a precessing magnetic field do not obey the selection rules associated with states of good z component of angular momentum. One therefore sees many interesting transitions that are forbidden in a static magnetic field.

The experiments in this work were performed with the focusing atomic beams machine built by Lemonick, Pipkin, and Hamilton.[9] K^{39} served as a convenient isotope for study.

The Hamiltonian of an atom subject to a static magnetic field, H_c, in the z direction and to several magnetic fields, $H_{\rm rot}{}^i$, rotating about the z axis may be written in the form[10]

$$H=H_F+g_J\mu_0 J_z H_c+g_J\mu_0 \times\sum_i H_{\rm rot}{}^i(J_x\cos\omega_i t+J_y\sin\omega_i t). \quad (1)$$

The rotating magnetic vectors, $H_{\rm rot}{}^i$, have been chosen in phase at $t=0$ for simplicity. Terms involving the interaction of the magnetic dipole moment of the nucleus with external magnetic fields have been neglected. H_F is the Hamiltonian of the hyperfine interaction in the absence of external fields.

$$H_F=A\mathbf{I}\cdot\mathbf{J}+B \times\left\{\frac{\frac{3}{2}(\mathbf{I}\cdot\mathbf{J})(2\mathbf{I}\cdot\mathbf{J}+1)-I(I+1)J(J+1)}{2I(2I-1)J(2J-1)}\right\}. \quad (2)$$

Magnetic octupole and higher order terms have been neglected in (2).

A transformation to a system of coordinates rotating with frequency ω_0 may be effected by means of the unitary transformation.[11]

$$U=e^{iF_z\omega_0 t}. \quad (3)$$

The transformed Hamiltonian is then

$$W=W_0+W_1=H_F+g_J\mu_0 J_z H_c-\omega_0 F_z+g_J\mu_0 \times\sum_i H_{\rm rot}{}^i\{J_x\cos(\omega_i-\omega_0)+J_y\sin(\omega_i-\omega_0)t\}, \quad (4)$$

* This work was supported by the U. S. Atomic Energy Commission.

[1] L. Grabner and V. Hughes, Phys. Rev. **82**, 561 (1951).
[2] J. Winter, thesis, Paris, 1958 (unpublished).
[3] C. Besset, J. Horowitz, A. Messiah, and J. Winter, J. Phys. Radium **15**, 251 (1954).
[4] H. Salwen, Phys. Rev. **99**, 1274 (1955).
[5] M. N. Hack, Phys. Rev. **100**, 975A (1955); thesis, Princeton University, 1955 (unpublished).
[6] J. E. Blamont and J. Winter, Compt. Rend. **244**, 332 (1957).
[7] W. Franzen and M. Alam, Phys. Rev. **133**, A460 (1964).
[8] E. Majorana, Nuovo Cimento **9**, 43 (1932).
[9] A. Lemonick, F. M. Pipkin, and D. R. Hamilton, Rev. Sci. Instr. **26**, 1112 (1955).
[10] H. B. G. Casimir, *On the Interaction between Atomic Nuclei and Electrons* (W. H. Freeman and Company, San Francisco and London, 1963).
[11] I. I. Rabi, N. F. Ramsey, and J. Schwinger, Rev. Mod. Phys. **26**, 167 (1954).

where hereafter the first three, time-independent terms will be denoted by W_0 and the terms representing rotating magnetic fields will be called W_1.

If only one rotating magnetic field, $H_{\rm rot}{}^1$, is present the transformed Hamiltonian W, Eq. (4) becomes time-independent when $\omega_1=\omega_0$. One may think of the rotating magnetic field as being attached to the x axis of the rotating coordinate system. W then assumes the form

$$W=W_0+g_J\mu_0H_{\rm rot}{}^1J_x. \tag{5}$$

The eigenvalue equation for the Hamilton of Eq. (5) is

$$W\phi_i=E_i\phi_i. \tag{6}$$

It is instructive at this point to use a perturbation argument to demonstrate the main features of the solutions of (6). We shall therefore consider the term $g_J\mu_0H_{\rm rot}J_x$ in (5) to be a small perturbation on the unperturbed Hamiltonian W_0, whose eigenvectors and eigenvalues are given by

$$W_0\psi(F,m)=\{E(F,m)-m\omega_0h\}\psi(F,m). \tag{7}$$

The $E(F,m)$ are the usual energies of the hyperfine sublevels in a magnetic field and the $\psi(F,m)$ are the corresponding eigenfunctions. F denotes the total angular momentum of the hyperfine level from which the eigenvalues evolve with increasing static magnetic field, and m is the z component of angular momentum of the eigenfunctions. Figure 1(a) shows a sketch of the eigenvalues of W_0 as a function of the frequency, ω_0, of the rotating coordinate system. As an example we have used the ground state of K^{39}, $I=\frac{3}{2}$, $J=\frac{1}{2}$, and only the sublevels originating from the $F=2$ level are drawn.

If we now apply the perturbation $H_{\rm rot}{}^1$ (5) the eigenvalues of W no longer intersect as in Fig. 1(a), but repel each other through the interaction caused by $H_{\rm rot}{}^1$, giving the situation sketched in Fig. 1(b). The continuous lines in Fig. 1(b) are labeled a through e in order of decreasing energy. They are eigenvalues of the states ϕ_i, which also vary continuously with ω_0. The ϕ_i do not possess a definite z component of angular momentum, and in fact for small values of $H_{\rm rot}{}^1$ ϕ_a's dominant m is $+2$ for $\omega_0=0$ and -2 for ω_0 very large. Near the region of intersections ϕ_a contains considerable admixtures of all magnetic quantum numbers. Two intersecting levels will repel most strongly when their z components of angular momentum differ by one unit. From the point of view of perturbation theory, states that differ by more than one unit in m repel through intermediate states so that relatively greater values of $H_{\rm rot}{}^1$ are required to split the intersections.

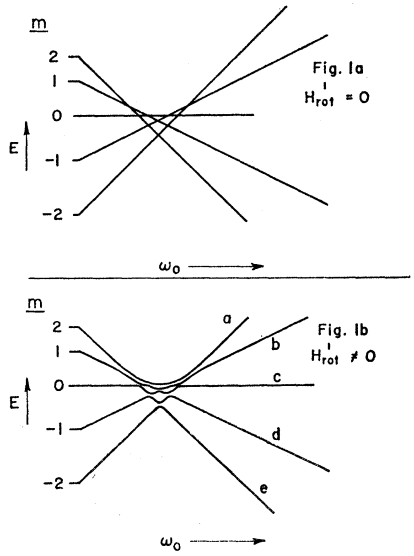

FIG. 1. Stationary states in a rotating coordinate system for K^{39}, $F=2$ (schematic). (a) No rf field. (b) A small magnetic field, $H_{\rm rot}{}^1$, is attached to the x axis of the rotating coordinate system.

TRANSITION INDUCING RF FIELD

Single-frequency transitions between two hyperfine levels can occur at the frequency of intersection of the corresponding asymptotes in Fig. 1(a).[3-5] One may also induce transitions between the steady states sketched in Fig. 1(b) by applying a second rf field, $H_{\rm rot}{}^2$, rotating around the static magnetic field. In view of (4) this second rf field can cause transitions between two levels i and j of Fig. 1(b) whenever

$$|W_i-W_j|=|\nu_2-\nu_1|. \tag{8}$$

ν_1 is the frequency of the large rotating magnetic field which defines the stationary states and ν_2 is the frequency of the small "tickling" field which causes transitions between the levels without significantly perturbing the term values. A second rf magnetic field oscillating along the direction of the static field can cause transitions at the frequency

$$|W_i-W_j|=\nu_2. \tag{9}$$

The former type of transition (8) was used in these experiments.

Whereas the Bohr frequency condition (8) must hold for any direct transition, selection rules often further limit the number of observable transitions. In a static magnetic field the z component of angular momentum is a good quantum number and the following selection rules arise for transitions between states $|i\rangle$ and $|j\rangle$ caused by a magnetic field rotating with frequency ν about the z axis

$$|m_i-m_j|=1, \tag{10}$$

$$\text{if}\quad m_i-m_j=1, \qquad \nu=+(W_i-W_j), \tag{11}$$

$$\text{if}\quad m_i-m_j=-1, \qquad \nu=-(W_i-W_j). \tag{12}$$

Had the states $|i\rangle$ and $|j\rangle$ been eigenstates ϕ of W (6), the preceding selection rules would not apply because the ϕ's are not in general states of definite z component of angular momentum. The relaxation of the selection rules (10), (11), and (12) in a precessing magnetic field has several interesting consequences. Both senses of

rotation, $\nu_2-\nu_1=\pm|W_i-W_j|$, of the transition inducing field can cause transitions between the stationary states in a precessing magnetic field. The two frequencies, ν_2' and ν_2'', at which a transition can occur satisfy the obvious relation [see Eq. (8)]

$$\nu_2'+\nu_2''=2\nu_1. \tag{13}$$

We have called a pair of lines corresponding to ν_2' and ν_2'' mirror lines because of their symmetry on a graph of ν_2 versus $H_{\rm rot}{}^1$. At least one of the mirror lines is forbidden for small $H_{\rm rot}{}^1$ where the selection rules (11) and (12) are still approximately true. Further discussion of mirror lines will be found in the following sections.

While the perturbation arguments outlined above are useful in visualizing the solutions to (6), interpretation of the data obtained in the present experiments requires an exact solution of the problem. This may be obtained by diagonalizing the Hamiltonian matrix of W, (5), in a suitable basis system. As basis vectors we have chosen the $\psi(F,m)$ in Eq. (7). The Hamiltonian matrix is then

$$\begin{aligned} hW_{F'm';Fm}&=(\psi(F'm'),W\psi(F,m))\\ &=(E(F,m)-\omega_0 m)\delta_{FF'}\delta_{mm'}\\ &\quad+g_J\mu_0 H_{\rm rot}{}^1(\psi(F'm'),J_x\psi(F,m)). \end{aligned} \tag{14}$$

When the zero-field hyperfine splitting is not too small a good approximation is to limit the matrix to one F level, thereby reducing the dimensionality from $(2I+1)\times(2J+1)$ to $(2F+1)$. Although this limitation is not necessary in principle, for large I and J considerable economy may be obtained without introducing significant errors. Figure 2 shows eigenvalues obtained by diagonalizing $W_{F'm';Fm}$ in the $F=2$ subspace. One should compare Fig. 2 with the schematic plots on Fig. 1 which were obtained by perturbation arguments. Figure 3 shows the dependence of the term values on the strength of the rotating magnetic field, $H_{\rm rot}{}^1$, for a fixed frequency, ν_1. The Princeton 7090 computer was used to obtain the wave functions $\psi(F,m)$ and eigenvalues

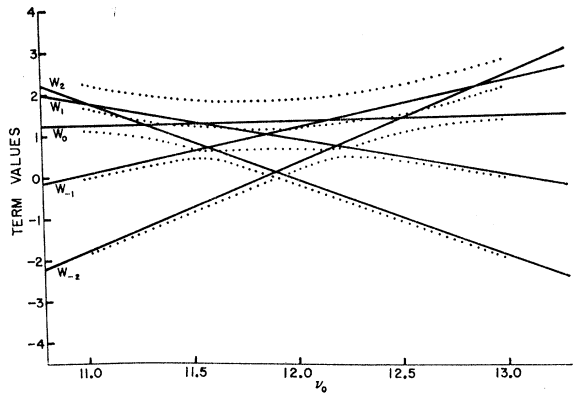

FIG. 2 Calculated term values (dotted lines) for $H_c=17$ G, $H_{\rm rot}=0.5$ G for K^{39}, $F=2$.

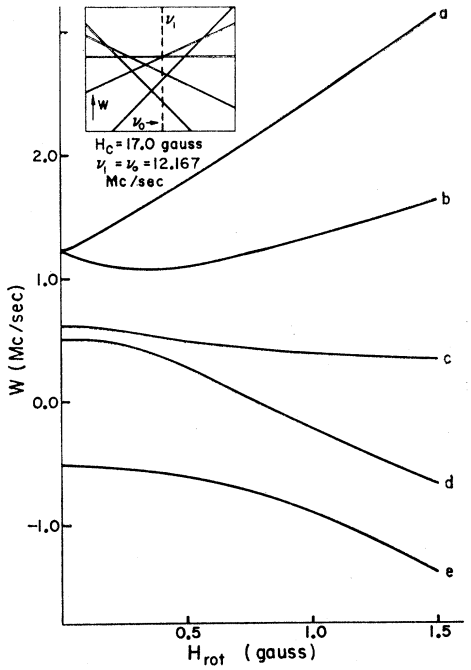

FIG. 3. Calculated term values as a function of the rotating magnetic-field strength. The inset shows the frequency ν_1 of the rotating magnetic field with respect to the term value diagram of Fig. 2.

$E(F,m)$ of (7), to compute the matrix elements $W_{mm'}$ of (14) and to diagonalize $W_{mm'}$.[12]

III. EXPERIMENTAL

Experimental work was performed with a focusing atomic beams apparatus designed by Lemonick, Pipkin, and Hamilton.[7] The beam of K^{39} normally used to calibrate the C magnet in studies of radioactive nuclei provided a convenient isotope for the experiments. Figure 4 shows a sketch of the rf loops in the C magnet.

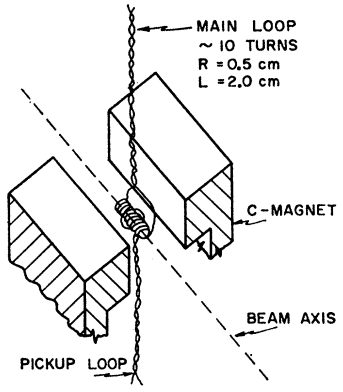

FIG. 4. The region of the atomic-beam machine where transitions occur.

[12] W. Happer, thesis, Princeton University, 1964 (unpublished).

These produce an oscillating rather than a rotating magnetic field, but since an oscillating field is composed of two rotating fields of frequencies $\pm\nu$ we can use one of the components and neglect the other. It will be seen that no significant effects arise from the opposite sense of rotation in these experiments. Two Rhode Schwartz type SMLR signal generators provided rf frequencies ν_1 and ν_2. A strong rf signal of frequency ν_1 served to define the stationary states and was applied to the 10 turn main loop (Fig. 4) normally used to induce multiple quantum transitions in studies of radioactive atoms. A Boonton type 230 A rf amplifier was occasionally used in conjunction with the Rhode Schwartz to obtain higher rf powers in the main loop. The rf voltage was displayed on a calibrated oscilloscope from which readings of rf field strength could be obtained. The small "tickling" rf signal, ν_2, was applied to a pickup loop which is normally used to monitor the rf field strength in the main loop. The field strength in the tickling loop was set to be $\sim\frac{3}{4}$ optimum for the $m=-1\rightarrow m=-2$ K^{39} transition with no signal present on the main loop. Moderate variations in the magnetic-field strength from the tickling loop are unimportant.

Machine optics are such that transitions into the level $m=-2$ are visible.[9] All of the transitions indicated in Fig. 5 therefore end on a line that evolves adiabatically from the -2 asymptote for smoothly increasing $H_{\rm rot}{}^1$.

Data were obtained by setting the first oscillator at a given frequency ν_1 and at a given rf field strength $H_{\rm rot}{}^1$. The frequency ν_2 of the "tickling" oscillator was then varied and the resonant frequencies recorded. The position of maximum flop was taken to be resonant frequency and this could be read to about ± 8 kc/sec. All frequencies were read on the dials of the respective oscillators and corrected later from calibration curves obtained with a Hewlett Packard model 524B signal counter. The corrected frequencies are probably good to about ± 15 kc/sec.

The rapid saturation of linewidths in an atomic beams apparatus, which arises from the smooth rf envelope seen by an atom,[2,13] is a considerable advantage in these experiments since the linewidths of the single-frequency transitions do not become broad enough to overlap even at very high rf fields. Similar experiments with an optically pumped vapor serving as a detector of rf transitions would be limited to smaller rf fields since the adiabatic application of rf power characteristic of a beams machine does not usually obtain.[2] The rectangular rf envelope seen by optically oriented atoms would cause multiple quantum transitions to overlap for large rf fields.

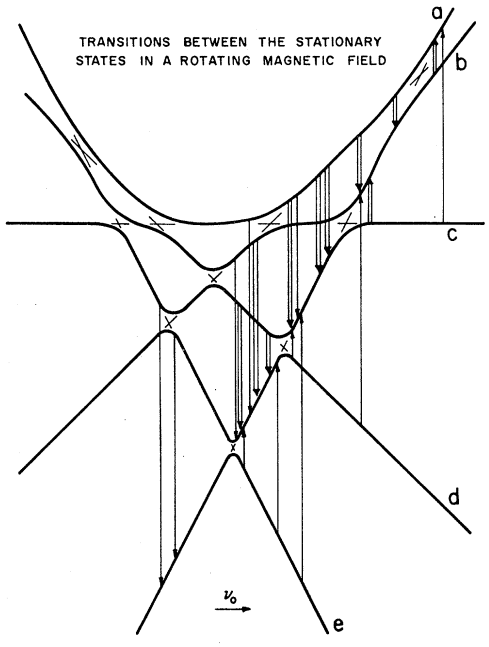

FIG. 5. Schematic diagram of the transitions which were observed in this work. Double arrows indicate observed mirror transition frequencies.

IV. RESULTS

Figure 6 shows the resonances seen when ν_1 was varied across the whole region of crossings. A point indicates that a resonance was observed at that combination of frequencies, ν_1 and ν_2 given on the axes. The strength of the rf field, $H_{\rm rot}{}^1$, varied continuously from ~ 2 G at $\nu_1=11.5$ Mc/sec to ~ 0.5 G at $\nu_1=13.8$ Mc/sec. The variation in rf field was unintentional. The transitions responsible for the resonances in Fig. 6 are labeled by the initial and final states involved. For example, the line *ca* in the lower right of Fig. 6 reflects a transition from level *c* to level *a* and is represented by the rightmost arrow in Fig. 5. A double line on Fig. 5 indicates an observed mirror pair of transitions. Positive identifica-

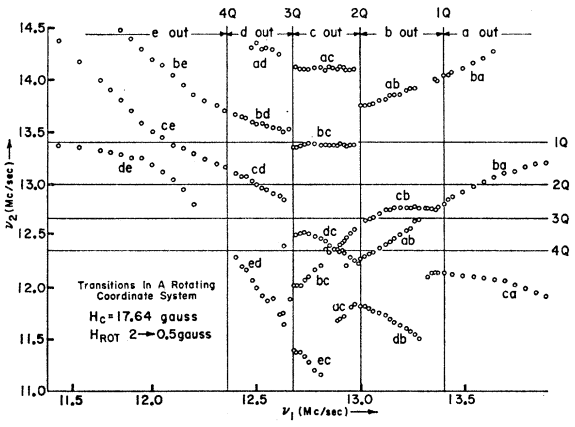

FIG. 6. Experimentally observed transitions in the frequency range of crossing levels. The state to which detectable transitions can be made is indicated on top of the figure. The single rf field transition frequencies are denoted $1Q\cdots 4Q$ for the one quantum through four quantum transitions, respectively.

[13] P. Kusch, Phys. Rev. **101**, 627 (1956).

tion of the lines in Fig. 6 was obtained from a study of their dependence on the magnetic-field strength H_{rot}[1], although several lines can be identified immediately. The line that approaches $1Q$ frequency to the right of the -1, -2 crossing must arise from the transition *ba* since no other visible transition can approach a constant frequency in that region. We may similarly identify *de* on the left of Fig. 6. Mirror lines (see Sec. III) can be identified on Fig. 6 by looking for pairs of lines ν_2' and ν_2'' such that $\nu_2'+\nu_2''=2\nu_1$. One can thus find the mirror pairs *ba* to the right of $1Q$, *ab* between $2Q$ and $1Q$, and *ac* and *bc* between $3Q$ and $2Q$. One should note the discontinuities in the lines on Fig. 6 approximately at the positions of single frequency resonances with ν_1. Reference to Fig. 5 shows that the final state which is flopped out changes abruptly from one continuous line to another when a single-field transition frequency is crossed. We have indicated the states which are flopped out on the top of Fig. 6. The right most discontinuity does not coincide with $1Q$ frequency because of a slight inhomogeneity in the C magnet.[12] Similar but successively smaller shifts of the discontinuity may be seen at the $2Q$ and $3Q$ transition frequencies. The lines *de* and *ce* on the left of Fig. 6 appear to approach and repel each other. This is understandable from Fig. 5 where we see *c* and *d* repelling at the -1, $+2$ crossing.

Figures 7(a)–7(i) show plots of transition frequency ν_2 for the tickler loop versus rf magnetic field in the main loop. The solid lines were calculated by the procedure outlined at the end of Sec. II and the points were measured as discussed in Sec. III. The solid lines should not be thought of as a "fit" since all parameters used in the calculation, the C field strength, the frequency of the signal on the main loop and the hyperfine structure constants of K^{39} were well known. However, only the relative strength of the rf field in the main loop was known experimentally so the horizontal scale of the experimental curves was adjusted to match the calculated lines. The insets in Figs. 7(a)–7(i) show the location of the frequency of the main loop with respect to the crossing points. Figure 5 is an expanded view of the insets. ν_1 was set at various frequencies starting from the -1, $+2$ crossing to slightly beyond the -2, -1 crossing. The agreement between experimental and theoretical curves is generally very good, but slight systematic deviations are visible in several cases. In Fig. 7(a) the experimental points seem consistently higher than the calculated curve *de*. In Fig. 7(b) the experimental points are systematically above *ce* and *de*. In Fig. 7(h) the experimental points are above *db*. These derivations may have arisen from poor calibration of the Rhode Schwartz frequency scales, from slight errors in the measurement of the C field, H_c, or the main frequency ν_1. They may also reflect the influence of the reverse rotating magnetic field from the main loop (Bloch-Siegert pulling[14]) or they may arise from the $F=1$ levels which were neglected in the diagonalization of the Hamiltonian matrix (14). Symmetrical mirror

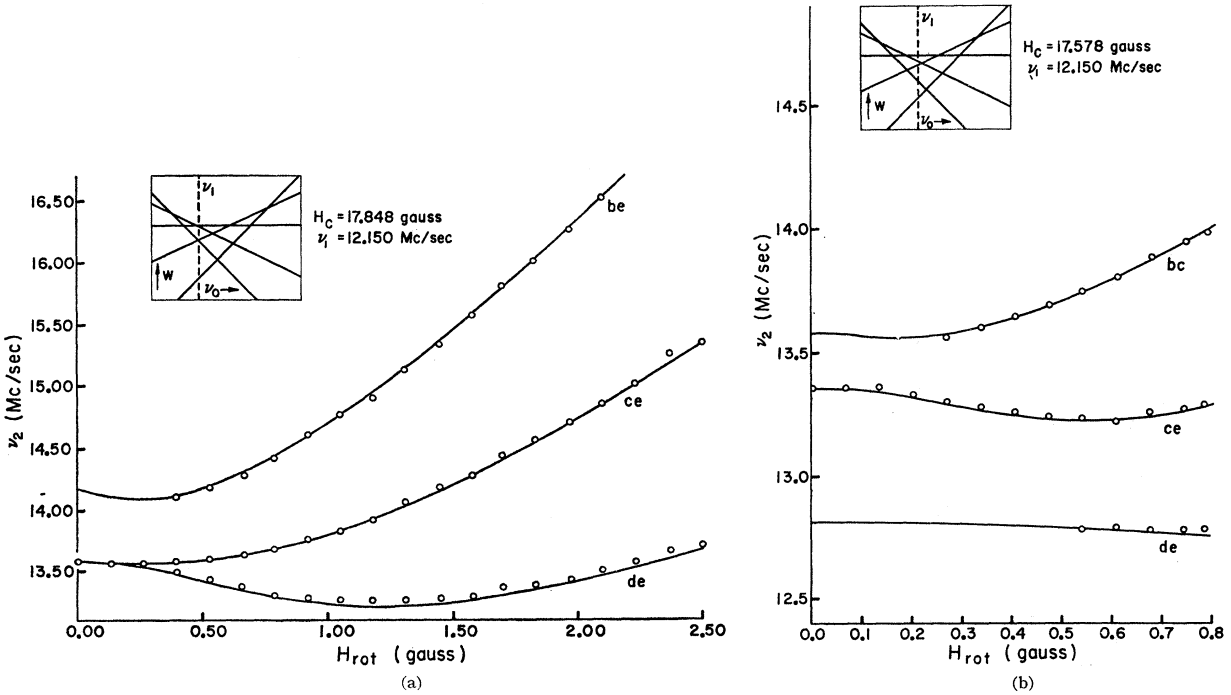

FIG. 7.—*Continued on next page.*

[14] F. Bloch and A. Siegert, Phys. Rev. **57**, 522 (1940).

lines are visible in Figs. 7(d)–7(i). In Fig. 7(e) ν_1 was set on the 0, −1 crossing so the transitions *ad* and *bd* are degenerate in the static field where they coincide with the normal one quantum transition. Note that transitions to level *d* are visible from all of the other levels, *a*, *b*, *c*, and *e*. Only *ad* and *bd* are allowed in the static field and the appearance of *ed*, the mirror pair *cd*, and the lower mirror line *bd* reflects the loss of axial symmetry in the stationary states. Similar considerations hold for the other figures. In Fig. 7(i) the mirror pair *ba* reflects the almost linear splitting of the levels *b* and *a* at the −1, −2 crossing. Good agreement could have been obtained in this case by a perturbation calculation. The splitting of the levels *b* and *a* is the only linear for

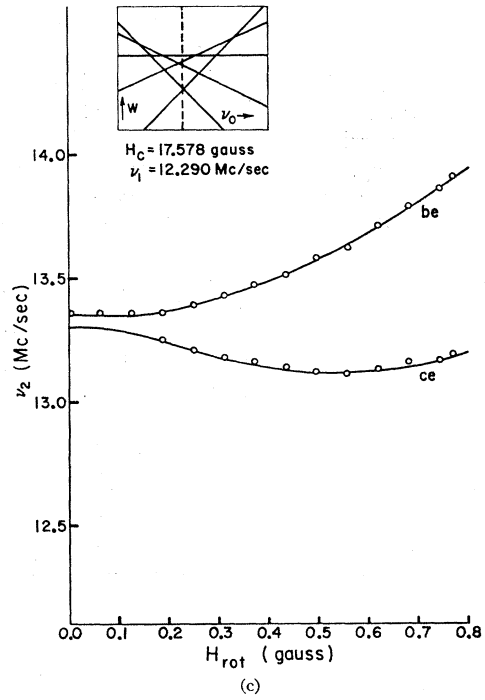

(c)

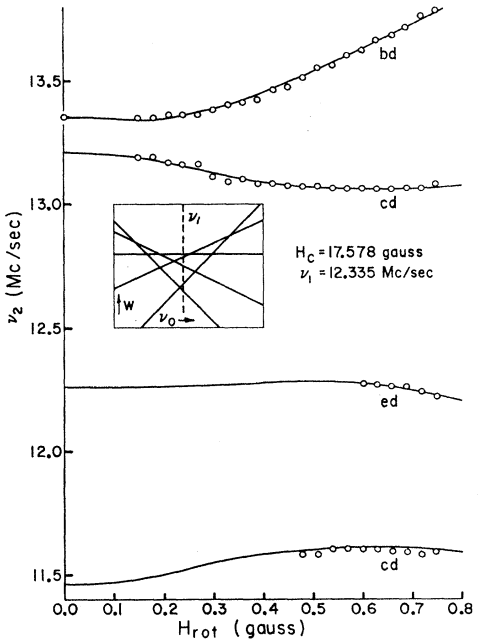

(d)

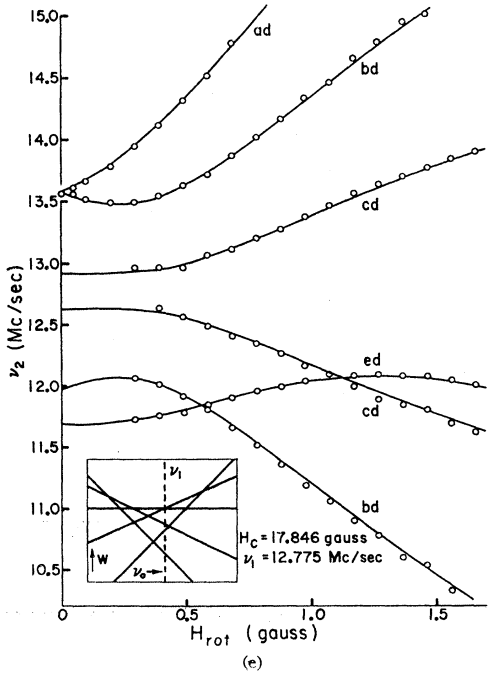

(e)

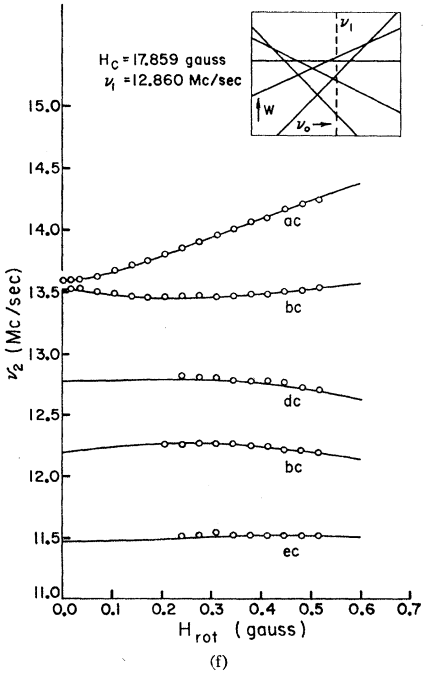

(f)

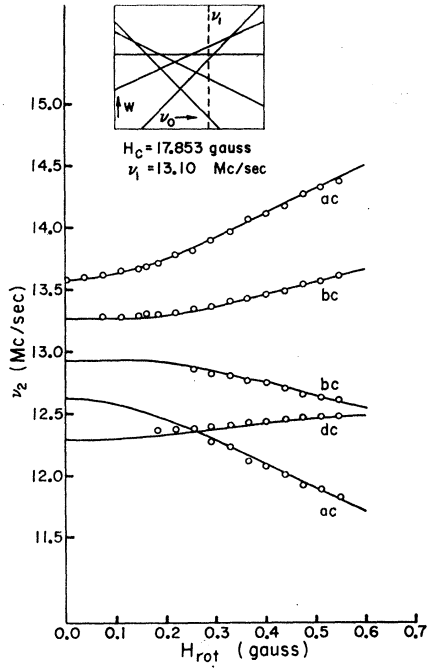

(g)

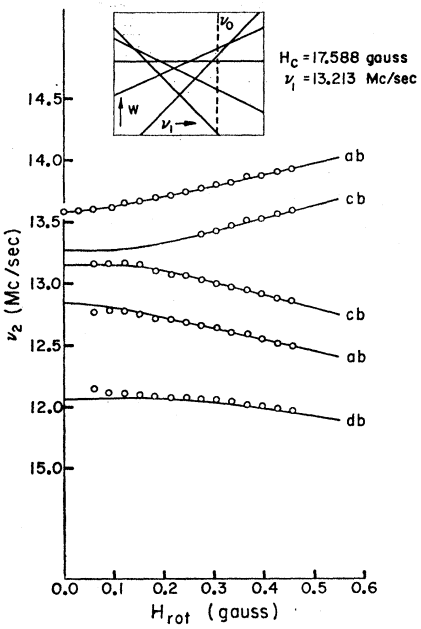

(h)

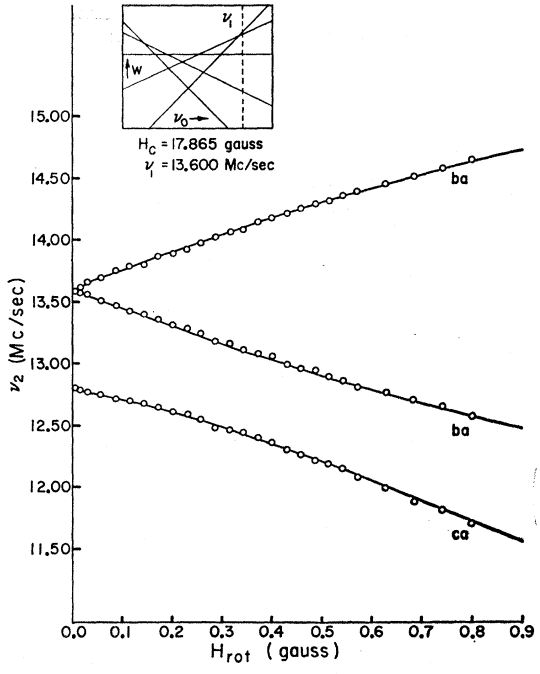

(i)

FIG. 7. Transition frequencies as a function of rotating magnetic-field strength. The solid lines are calculated; the circles are experimental points. The insets show the frequency ν_1 of the rotating magnetic field with respect to the term value diagram of Fig. 2. Mirror lines are visible in (d) through (i).

much smaller values of $H_{\rm rot}^1$ in Fig. 7(e) because of the proximity of other levels. The final state d is also rapidly shifted as is evident from the term value diagram, Fig. 3, which approximates the situation of Fig. 7(e). Thus a perturbation calculation here would be of very limited value.

The experiments above constitute a measurement of rf magnetic fields. The same degree of accuracy can be obtained as is usually obtained in the measurement of the C field with a calibrating isotope. The uncertainty in the measurement is determined by the linewidth of the resonance. For example, the splitting at the -2, -1

crossing may be calculated by perturbation theory to be $\Delta\nu = W_a - W_b = 0.701 H_{rf}$ Mc/G for H_{rf} small. The uncertainty in the measured rf field is then $\delta H_{rf} = 1.43\delta(\Delta\nu)$ G/(Mc/sec). One can determine the center of our K^{39} lines to about 1 kc/sec or $\delta(\Delta\nu)$ to about 2 kc/sec which would give an uncertainty in measured rf field of about 0.003 G. For comparison, optimum power for a one quantum transition is $\sim$0.02 G.

Measurements of rf magnetic fields are sometimes made relative to optimum power for some transition. However, determination of the actual rf magnetic field in gauss which corresponds to optimum power requires a knowledge of the velocity distribution of the atoms. The method outlined above is independent of the velocity distribution of the atoms and may in fact be used in conjunction with a measurement of optimum power to determine the velocity of the atoms in an almost monochromatic beam. The shape of the rf envelopes should be taken into account in any calculations of rf magnetic-field strengths.

ACKNOWLEDGMENTS

The author would like to thank Professor D. R. Hamilton, Professor J. D. McCullen, and Professor O. Ames for their interest in this work and for useful discussions. He also wishes to thank R. G. Cornwell for facilitating the atomic-beam experiments.

PHYSICAL REVIEW VOLUME 136, NUMBER 1A 5 OCTOBER 1964

Two-Photon Processes in Complex Atoms*

J. D. Axe, Jr.
IBM Watson Research Center, Yorktown Heights, New York
(Received 15 May 1964)

The off-diagonal matrix elements of the polarizability operator when operating within an l^N configuration of a complex atom can be approximately written in simple tensor-operator form. The resulting expressions are discussed in terms of two-photon absorption and the recently observed electronic Raman scattering in the trivalent rare-earth ions.

I. INTRODUCTION

THE extremely intense light fluxes available from optical maser sources have revived interest in interactions in which atomic matter and two or more quanta of electromagnetic energy are involved.[1] The most easily observable two-photon effects, Rayleigh and Raman scattering, were given modern quantum-mechanical treatment by Dirac.[2] Two-photon absorption and emission, also predicted by second-order perturbation theory, were first discussed by Goeppert-Mayer.[3]

Of the recently investigated two photon effects at optical frequencies, several have occurred in systems which to a good approximation can be described as free atoms. Thus, two-photon absorption has been observed by Kaiser and Garrett[4] in Eu^{2+} in a matrix of CaF_2, and in atomic Cd vapor by Abella.[5] The first observed atomic Raman transitions were reported recently by Hougen and Singh.[6] Sorokin and Braslau[7] have recently suggested the possibility of producing stimulated two-photon emission at optical frequencies by triggering with intense light at the subharmonic frequency. In view of the possible importance of such processes, the purpose of the present paper is to examine the second-order perturbation expansions which determine two-photon interaction in complex atoms in the hope of developing approximate expressions more amenable to both qualitative and quantitative evaluation. The development is similar in spirit to the polarizability approximation introduced by Placzek[8] and others for treating vibrational and rotational Raman transitions.

II. FORMULAS AND APPROXIMATIONS

Consider an atomic system in an eigenstate β but with other allowed eigenstates β', β'', etc., upon which monochromatic light of frequency ω_1 is incident. The result of the second-order electric-dipole-interaction perturbation[2] can be summarized by attributing to the atomic system induced-oscillator dipole moments with (complex) amplitudes of the form

$$(\beta' | \mathbf{P}(\omega_2) | \beta) = (\beta' | \boldsymbol{\alpha} | \beta) \cdot \mathcal{E}(\omega_1),$$

where $\mathcal{E}(\omega_1)$ is the electric field associated with the incident radiation and the oscillator frequencies ω_1 and ω_2

* This research has been supported in part by the U. S. Army Research Office, Durham, North Carolina.

[1] See, for example, J. A. Armstrong, N. Bloembergen, J. Ducuing, and P. S. Pershan, Phys. Rev. 127, 1918 (1962).

[2] P. A. M. Dirac, Proc. Roy. Soc. (London) A114, 143, 710 (1927).

[3] M. Goeppert-Mayer, Anw. Physik 9, 273 (1931).

[4] W. Kaiser and C. G. B. Garrett, Phys. Rev. Letters 7, 229 (1961).

[5] I. D. Abella, Phys. Rev. Letters 9, 453 (1962).

[6] J. T. Hougen and S. Singh, Phys. Rev. Letters 10, 406 (1963).

[7] P. P. Sorokin and N. Braslau, IBM J. Res. Develop. 8, 177 (1964).

[8] G. Placzek, *Handbuch der Radiologie* (Akademische Verlagsges, Leipzig, 1934), Vol. 6, Part 2, p. 205.